



HAL
open science

The miR 302-367 cluster drastically affects self-renewal and infiltration properties of Glioma-initiating cells through CXCR4 repression and consequent disruption of the SHH-GLI-NANOG network

Thierry Virolle, Mohamed Fareh, Laurent Turchi, Virginie Virolle, David Debruyne, Philippe Paquis, Olivier Preynat-Seauve, Karl-Heinz Krause, Hervé Chneiweiss, Fabien Almairac, et al.

► To cite this version:

Thierry Virolle, Mohamed Fareh, Laurent Turchi, Virginie Virolle, David Debruyne, et al.. The miR 302-367 cluster drastically affects self-renewal and infiltration properties of Glioma-initiating cells through CXCR4 repression and consequent disruption of the SHH-GLI-NANOG network. *Cell Death and Differentiation*, 2011, 10.1038/cdd.2011.89 . hal-00655645

HAL Id: hal-00655645

<https://hal.science/hal-00655645>

Submitted on 1 Jan 2012

HAL is a multi-disciplinary open access archive for the deposit and dissemination of scientific research documents, whether they are published or not. The documents may come from teaching and research institutions in France or abroad, or from public or private research centers.

L'archive ouverte pluridisciplinaire **HAL**, est destinée au dépôt et à la diffusion de documents scientifiques de niveau recherche, publiés ou non, émanant des établissements d'enseignement et de recherche français ou étrangers, des laboratoires publics ou privés.

The miR 302-367 cluster drastically affects self-renewal and infiltration properties of Glioma-initiating cells through CXCR4 repression and consequent disruption of the SHH-GLI-NANOG network

running title

The miR 302-367 cluster as tumor suppressor

MOHAMED FAREH¹, LAURENT TURCHI¹, VIRGINIE VIROLLE¹, DAVID DEBRUYNE¹, FABIEN ALMAIRAC^{1,4}, STEPHANIE DE-LA-FOREST DIVONNE¹, PHILIPPE PAQUIS⁴, OLIVIER PREYNAT-SEAUVE³, KARL-HEINZ KRAUSE³, HERVÉ CHNEIWEISS² AND THIERRY VIROLLE¹⁻⁵.

1-INSERM U898/UNSA, Cellules Souches, Développement et Cancer, faculté de médecine, av valombrose, 06107 Nice, France

2-U894 Inserm/Université Paris-Descartes, Plasticité Gliale, Centre de Psychiatrie et Neurosciences, 2Ter rue d'Alésia 75014 Paris, France

3- Department of Pathology and Immunology, Faculty of Medicine, University of Geneva and Department of Genetic and Laboratory Medicine, Geneva Hospital, Switzerland.

4-service de Neurochirurgie, hôpital Pasteur, CHU de Nice, 06107, France

5-correspondences should be addressed to: TV

INSERM U898/UNSA, Cellules Souches, Développement et Cancer, faculté de médecine, av valombrose, 06107 Nice, France. Tel: 04 93 37 76 20, e-mail: virolle@unice.fr

Abstract

Glioblastoma multiforme (GBM) is the most common form of primary brain tumor in adults, often characterized by poor survival. Glioma initiating cells (GiCs) are defined by their extensive self-renewal, differentiation, and tumor initiation properties. GiCs are known to be involved in tumor growth and recurrence, and in resistance to conventional treatments. One strategy to efficiently target GiCs in GBM consists in suppressing their stemness and consequently their tumorigenic properties. Here, we show that the miR-302-367 cluster is strongly induced during serum-mediated stemness suppression. Stable miR-302-367 cluster expression is sufficient to suppress the stemness signature, self-renewal, and cell infiltration within a host brain tissue, through inhibition of the CXCR4 pathway. Furthermore, inhibition of CXCR4 leads to the disruption of the SHH-GLI-NANOG network, which is involved in self-renewal and expression of the embryonic stem cell-like signature. In conclusion, we demonstrated that the miR-302-367 cluster is able to efficiently trigger a cascade of inhibitory events leading to the disruption of GiCs stem-like and tumorigenic properties.

Introduction

Glioblastoma multiforme (GBM) is the most common form of primary brain tumor in adults, with a median survival rate of 14 months¹. The poor outcome of this disease is due to the aggressive nature of the tumor. In fact, GBM is a highly vascularized, diffuse and infiltrating tumor that can develop lesions at sites distant from the primary tumor². Conventional treatments for GBM consist of surgical resection followed by radiation and/or chemotherapy³ aimed at eliminating residual tumor cells that have infiltrated into the surrounding brain. Combined radiotherapy plus concomitant and adjuvant temozolomide was found to significantly increase survival¹, especially in patients exhibiting epigenetic silencing of the O-6 methylguanine-DNA methyltransferase (MGMT) gene⁴. However, such a therapeutic approach remains largely ineffective, and its failure exclusively leads to brain recurrences, both at the primary and distant sites. Failure to cure malignant gliomas has been attributed to the extensive resistance of glioma-initiating cells (GICs) to conventional cytotoxic therapies. Indeed, cytotoxic therapies efficiently target the rapidly proliferating tumor cells present in the tumor bulk, while they spare the slowly proliferating GICs compartment. The “GICs hypothesis” proposes that a minority of highly tumorigenic cells in the tumor bulk – originating from transformed stem cells, restricted progenitor, or more differentiated cells with acquired self-renewal and multipotent properties – are responsible for tumor initiation, development, and behavior⁵. The concept of tumor stem cells was originally proposed for myeloid leukemia⁶ and subsequently shown to be valid for solid tumors as well, as demonstrated in a mouse model of breast cancer⁷. Recently, cancer stem cells have been isolated from a variety of human solid tumors, and thereafter characterized⁸. Studies conducted in animal xenograft models provided strong evidence for the tumorigenic, self-renewal, and differentiation properties of GICs. In fact, such studies showed that as low as 100 GICs are able to induce growth of tumors exhibiting the same phenotypic heterogeneity as the original primary tumor⁹. Interestingly, a recent report showed that GICs become vulnerable to therapies, and more importantly lose their highly tumorigenic ability, when they are forced to mature into a more differentiated state¹⁰. Therefore, the identification of ways to efficiently affect GICs properties may lead to the development of new therapeutic approaches for the treatment of malignant glioma. In this context, it is crucial to investigate the mechanisms involved in GICs plasticity. Such a plasticity is mostly regulated by a tight epigenetic control of gene expression. Micro-RNAs modulate gene expression levels by promoting either inhibition of translation or mRNAs degradation. Undifferentiated human

embryonic stem cells express a miRNA signature that seems to be involved in controlling their self-renewal ability and pluripotency¹¹. Interestingly, inhibition of Dicer or Drosha, responsible for miRNA processing, alters self-renewal and differentiation of human embryonic stem cells¹².

In the present study, we show that the miR 302-367 cluster is rapidly and strongly induced in GiCs undergoing serum-mediated suppression of stemness. This miR cluster is undetectable in self-renewing GiCs; however, when stably and constitutively expressed, it is able to suppress the stemness gene signature, self-renewal, and cell infiltration through the inhibition of the CXCR4 pathway. In addition, we show that blockade of CXCR4 signaling leads to the disruption of the SHH-GLI-NANOG network, which is known to be responsible for self-renewal and expression of the ES-like genes signature in glioma cancer stem cells¹³.

Results

The miR-302-367 cluster contributes to serum-mediated loss of stemness

To identify miRNAs capable of suppressing GiCs stemness properties, we used two previously characterized GiCs primary lines¹⁴, TG1 and TG6, and took advantage of the ability of serum to induce stem cells differentiation¹⁴. Self-renewing TG cells were forced into a more differentiated non-stem-like state, by substituting the growth factors EGF and bFGF (necessary for self-renewal) with 0.5% serum. Four days following serum addition, the cells exhibited low levels of the stemness markers Oct-4 and Nanog, (supplementary Figure 1A), and of Sonic hedgehog (SHH) – a secreted protein clearly established as a major player in GiCs self-renewal¹⁵ (Figure 1A; Figure 1B, upper panel). In addition, the glial proteins GFAP and Olig2 were upregulated (Figure 1A; Figure 1B, upper panel). Consistent with SHH repression, serum treatment drastically reduced clonal proliferation (Figure 1B, lower panel). This first set of results confirmed that serum-treated TG cells are an ideal system to identify molecules involved in loss of stem-like properties. Hence, we compared the human miRNA signature of self-renewing TG1 and TG6 cells with that of 4-day serum-differentiated cells. Three independent experiments revealed about 60 miRNAs significantly modulated at this time point. Since our goal was to identify miRNAs able to promote loss of stemness, we took into account only the most up-regulated miRNAs and focused on the miR-302-367 cluster (Figure 1C) whose members (miR-302a, b, c, d, and miR-367) were exclusively expressed in serum-differentiated cells (Supplementary Figure 1B). A time course analysis revealed a clear induction of this cluster starting at day 1, and a maximal expression at day 3 (Figure 1D;

Supplementary Figure 1C), which was maintained up to 15 days following serum addition. Similar results were obtained using two additional GiCs primary lines, GB1 and #1056 (data not shown and Supplementary Figure 1D). In order to assess miR-302-367 cluster contribution in serum-mediated suppression of stemness, we transiently transfected TG1 cells with anti-miR-302a, anti-miR302b, or anti-miR-367 (Figure 1E), or with a pool of these 3 anti-miRs (Figure 1F). Twenty-four hours after transfection, the cells were treated with serum. QPCR analysis revealed that the aforementioned anti-miRs were able to reduce the expression of each miR by 50%, whether they were used individually or as a pool (Supplementary Figure 2A and B). While individual anti-miR did not affect the differentiation process (Figure 1E), the pool was able to significantly alter the expression of GFAP, Olig2, and SHH (Figure 1F), suggesting compensatory mechanisms. Altogether, these results demonstrate a functional contribution of the miR-302-367 cluster in serum-mediated suppression of stemness.

The miR-302-367 cluster promotes suppression of stemness and contributes to GiCs glial commitment

To assess the capacity of the miR-302-367 cluster to suppress stemness in the absence of serum, we ectopically expressed the four members of the miR-302-367 cluster in undifferentiated TG1 cells. First, we amplified the nucleotide sequences spanning the region containing the whole miR-302-367 cluster from genomic DNA. Then, we cloned this genomic region into a lentiviral vector. Finally, we used this construct to generate the TG1 Cluster 302 and TG6 Cluster 302#1 cell lines, which stably expressed each miR-302-367 cluster member (Figure 2A and B). As control, we used TG1 and TG6 cells expressing a non-relevant small non-coding RNA (TG1 and TG6 Ctrl cells). To assess the miR-302-367 cluster ability to trigger TG1 differentiation in the absence of serum, we cultured TG1 Ctrl and TG1 Cluster 302 cells in a minimum defined medium deprived of EGF and bFGF (NS34-), for 4 days. This medium is sufficient to maintain a stem-like state while preventing spontaneous differentiation of control cells. In these conditions, TG1 and TG6 Ctrl cells grew as non-adherent neurospheres (Figure 2A and B, left panels), while TG1 and TG6 Cluster 302 cells grew adherent to the dish and exhibited a non-stem-like differentiated phenotype (Figure 2A and B right, right panels). Accordingly, QPCR analysis showed an increased expression of GFAP and a reduced expression of SHH in the TG1 Cluster 302 and TG6 Cluster 302#1 as compared to the Ctrl cells (Figure 2C). To confirm these results at the protein level, we studied the expression of stemness markers by immunofluorescence. While the stemness markers SHH, Oct4, Nanog, and Sox1 were clearly expressed in TG1 Ctrl cells cultured in

growing medium (NS34+) (Figure 3A, upper panel), they were almost undetectable in TG1 Cluster 302 cells cultured under the same conditions (Figure 3A, lower panel). Interestingly, when TG1 Cluster 302 cells were cultured in NS34-, GFAP was strongly expressed (Figure 3B). In addition, unlike what was observed in cells treated with serum, neuronal markers such as NeuN remained undetectable (Figure 3B). Similar results were obtained using TG6 Cluster 302#1 cells (Supplementary Figure 3A, B and C). Altogether, these results clearly demonstrate that expression of the miR-302-367 cluster alone is sufficient, in a context favorable for GiCs self-renewal, to promote loss of stemness markers and to contribute, in quiescent conditions, to early tumor glial fate commitment.

miR-302-367 cluster expression drastically inhibits GiCs self-renewal and infiltration properties

The loss of stemness markers mediated by miR-302-367 cluster expression strongly suggests an impairment of stem-like properties. To further assess this hypothesis, we evaluated the clonal efficiency of TG1 Cluster 302 cells compared to TG1 Ctrl cells. Towards this goal, we seeded 10 cells/well in a 96 wells plate and considered clonal efficiency to be 100% when, after 1 month, 10 neurospheres were counted in a well. While 80% of single TG1 Ctrl cells were able to form neurospheres, less than 10% of TG1 Cluster 302 cells were able to do so (Figure 4A). In other words, miR-302-367 cluster inhibited clonal proliferation of more than 80% (Figure 4A). Similar results were obtained using TG6 Cluster 302#1 and TG6 Ctrl cells (Supplementary Figure 3D). Importantly, the size of the neo-formed neurospheres in TG1 Cluster 302 cells was much smaller than the one observed in TG1 Ctrl cells (Figure 4A), suggesting a reduction of the proliferation rate. To compare the cell cycle characteristics of TG1 Cluster 302 cells with those of TG1 Ctrl cells, we analyzed their cell cycle profiles by FACS (Figure 4B). When compared to TG1 Ctrl cells, TG1 Cluster 302 cells exhibited an accumulation of cells in the G1 phase (59.49% versus 51.76%). The lower proliferation rate of TG1 Cluster 302 cells was confirmed using proliferation assays (Figure 4C). To further assess the impact of such a growth impairment on the development of an *in vitro* 3D tumor-like cellular mass, we seeded TG1 Ctrl and TG1 Cluster 302 cells, previously labeled with the red fluorescent protein, on separate nylon filters in a minimum medium and under air-liquid interface conditions. After 1 month of growth in these conditions, a cellular mass can be visualized. Our results showed that TG1 Ctrl cells developed into a thick and compact tissue, while TG1 Cluster 302 cells failed to do so and appeared as a thin monolayer (Figure 4D). To further assess TG1 or TG6 Cluster 302 cells ability to infiltrate and proliferate within a host

cerebral tissue we used *ex-vivo* organotypic cultures of thick mouse brain slices (Figure 4E). We seeded red fluorescent TG Ctrl or TG Cluster 302 cells on the surface of mouse brain slices and allowed them to grow for 3 weeks. Subsequently, the cerebral sections were fixed, embedded in paraffin, and sliced. Since the cells were labeled with the red fluorescent protein, they could be easily visualized within the tissue. Our results showed a strong ability of Ctrl cells to infiltrate and proliferate within the cerebral tissue, initiating the development of a tumor-like mass in the vicinity of individual migrating cells (Figure 4E and Supplementary Figure 3E). Conversely, TG Cluster 302 cells failed to penetrate the tissue and remained on the surface of the brain slice (Figure 4E and Supplementary Figure 3E). Under certain circumstances, lack of interaction with the brain tissue even led to loss of the cells (Figure 4E, lower panel – Block 2; Supplementary Figure 3E). In order to assess the tumorigenic potential of TG1 Ctrl and TG1 Cluster 302 cells *in vivo*, we performed intracranial xenografts in NOD/SCID mice using either TG1 Ctrl or TG1 Cluster 302 cells stably expressing a luciferase reporter gene. Prior to injection, the luciferase activity was assessed by an *in vitro* luciferase assay and was found to be equivalent in the two cell lines. Time course analysis following the xenograft showed that while TG1 Ctrl cells induced and maintained a tumor for at least 1 month, the TG1 Cluster 302 cells failed to do so. Taken together these results demonstrate that miR-302-367 cluster expression is sufficient to inhibit clonal proliferation and infiltration, therefore compromising GiCs tumorigenic properties.

miR-302-367 cluster expression leads to a drastic downregulation of CXCR4/SDF1

Over-expression of CXCR4, a strong tumorigenic and invasiveness marker, often characterizes neural cancer stem cells as well as many other cancer cells¹⁶. Interestingly, *in silico* analysis (Miranda, pictar vert) indicated that the CXCR4 3' UTR end as well as the 3' UTR end of its ligand CXCL12/SDF1 might be directly targeted by miR-302a, b, c, and d (Figure 6A). In order to assess whether this putative regulation occurs in our system, we transiently transfected TG1 cells with the miR-302-367 cluster and compared CXCR4 and SDF1 mRNA levels with those of TG1 cells transfected with a non-relevant construct. Our results indicated a strong miR-302-367 cluster-mediated inhibition of CXCR4 and SDF1 expression (Figure 6B). Accordingly, CXCR4 and SDF1 protein levels were significantly reduced in TG1 Cluster 302 cells when compared to TG1 Ctrl cells (Figure 6C and E). In addition, functional inhibition of at least two cluster members (302a and 302b) was sufficient to partially rescue CXCR4 and SDF1 expression in TG1 Cluster 302 cells (Figure 6C). Similar results were obtained using TG6 Ctrl and TG6 Cluster 302#1 cells (supplementary

Figure 4A and B). In order to assess whether the miR-302 directly mediates CXCR4 expression, we cloned the 3'UTR region of CXCR4 mRNA and fused it to a luciferase reporter gene; this construct was then transfected in 293T cells along with synthetic miR-302a or miR-23 (used as control non-relevant miR). Our results clearly showed a strong repression of luciferase activity only in the case of miR-302a (Figure 6D). This repression did not occur in the presence of miR-23 or when using a construct corresponding to the CXCR4 3'UTR lacking the miR-302a binding site. Therefore, these results argued for a direct role of miR-302 in the regulation of CXCR4 expression. Migration assays performed using Boyden chambers further confirmed CXCR4 inhibition in TG Cluster 302 cells, as no migration was observed in these cell lines (Figure 6F and supplementary Figure 4C). Interestingly, cell migration resumed when CXCR4 expression was restored by stable expression of a CXCR4 construct lacking the 3'UTR region (Supplementary Figure 4D). Taken together these results clearly demonstrate that the miR-302-367 cluster promotes strong functional inhibition of the CXCR4 pathway.

CXCR4 constitutes one of the major miR-302-367 cluster targets involved in the suppression of GiCs properties

To assess the effects of CXCR4 inhibition in TG1 cells, we used the non-peptide antagonist AMD3100 or an anti-CXCR4 blocking antibody to prevent the binding of ligands. Treated and untreated TG1 cells were then seeded on the surface of mouse brain slices to evaluate their infiltrative properties. While control untreated cells strongly and deeply interacted with the brain tissue, TG1 cells deficient of functional CXCR4 did not, and remained as non-adherent spheres (Figure 7). Interestingly, TG1 Cluster 302 cells behaved similarly and did not interact with the brain tissue (Figure 7). Importantly, analysis of paraffin sections revealed that only the control TG1 cells were able to infiltrate and migrate into the cerebral tissue (Figure 7). The fact that similar results were obtained using TG1 cluster 302 cells or TG1 cells treated with the non-peptide antagonist AMD3100 or with anti-CXCR4 blocking antibody demonstrated that the miR-302-367 cluster-mediated CXCR4 inhibition was the main regulatory mechanism required to suppress GiCs infiltrative properties. Since SDF1/CXCR4 has been described as a promoter of glioma cells proliferation¹⁷, we reasoned that the reduced clonal proliferation of TG Cluster 302 cells (Figure 4A and Supplementary Figure 3D) might also be the result of CXCR4 inhibition. Therefore, we performed clonal proliferation assays as previously described, using TG1 cells cultured either in their proliferation medium or in presence of anti-CXCR4 blocking antibody. Our results showed

that inhibition of the CXCR4 pathway led to a drastic loss of clonal efficiency (Figure 8A). We then sought to investigate the molecular mechanism behind the reduction of clonal proliferation induced by CXCR4 impairment. Since previous reports demonstrated that the SHH-GLI1-NANOG network is crucial for glioma cancer stem cells self-renewal and tumorigenic properties^{13,15,18,19}, we assessed the expression of this gene network in TG1 cells stably expressing the miR-302-367 cluster or grown in the presence of anti-CXCR4 blocking antibody or AMD3100. QPCR analysis revealed that stable expression of the miR-302-367 cluster or functional inhibition of CXCR4 caused reduction of both SHH and GLI1 expression (Figure 8B). Consistently, while SHH and NANOG were clearly detected in control cells by immunofluorescence, they were almost undetectable in cells with impaired CXCR4 function and in cells stably expressing the miR-302-367 cluster (Figure 8C). Consistent with the drastic loss of clonal proliferation (Figure 8E), PBK/TOPK kinase and its substrate (the histone H3 ser10), which are expressed and phosphorylated in dividing cells, were also suppressed (Figure 8F). Interestingly, the restoration of CXCR4 expression by stable over-expression of a CXCR4 construct lacking the 3'UTR region, rescued both SHH and NANOG protein expression, the Hedgehog pathway, as well as 50% of PBK/TOPK and histone H3 ser10 expression, and therefore a part of TG1 Cluster 302 cells clonal proliferation (Figure 8B, D, E, and F). These results revealed that a functional CXCR4 pathway is necessary to maintain the SHH-GLI1-NANOG network and self-renewal properties. In addition, they revealed the strong ability of the miR-302-367 cluster to disrupt the SHH-GLI1-NANOG network, in part through CXCR4 inhibition. In another set of experiments, we restored SHH expression in TG1 cells either impaired for CXCR4 function or stably expressing the miR-302-367 cluster using an exogenous recombinant protein. Such cells were then examined for their clonogenicity. Our results clearly showed that exogenous recombinant SHH was able to increase clonal proliferation of cells lacking functional CXCR4 (Figure 8E). However, exogenous recombinant SHH failed to rescue clonal proliferation of TG1 cells stably expressing the miR-302-367 cluster (Figure 8E). Exogenous recombinant SHH was therefore sufficient to bypass CXCR4 inhibition, confirming the importance of this pathway in the control of self-renewal. The fact that recombinant SHH had no effect on cells stably expressing the miR-302-367 cluster suggests a strong ability of these miRs to inhibit multiple pathways involved in cell proliferation. Interestingly, a recent report and in silico analyses have identified various proteins involved in the regulation of cell cycle progression – specifically, E2F1, Cyclin A (CyA) and Cyclin D1 (CyD1) – as direct targets of the miR-302-367 cluster²⁰. Therefore, we assessed the expression of such proteins in TG1 cells lacking

functional CXCR4 or stably expressing the miR-302-367 cluster. QPCR analysis revealed that expression of the miR-302-367 cluster caused a drastic downregulation of E2F1, CyA, and CyD1 mRNA levels, while CXCR4 inhibition did not (Figure 8G). Altogether, these results demonstrate that expression of the miR-302-367 cluster compromises both cell infiltration and self-renewal properties by inducing a cascade of inhibitory events leading to CXCR4 repression and consequent disruption of the SHH-GLI1-NANOG network. In addition, they demonstrate that the miR-302-367 cluster is able to directly interfere with the expression of proteins of the cell cycle machinery.

Discussion

GiCs represent an attractive target for the treatment of high-grade brain tumors such as GBM. A possible approach to target GiCs consists in forcing them into a more differentiated phenotype characteristic of the tumor bulk¹⁰. By taking advantage of serum-induced differentiation and loss of stemness, we demonstrated the ability of the miR-302-367 cluster to compromise the maintenance of stem-like TG1 cells and to reduce their infiltration within a host cerebral tissue. Indeed, constitutive and stable expression of the miR-302-367 cluster was sufficient to strongly inhibit the clonogenicity of stem-like TG1 cells and to promote loss of proteins characteristic of their stem-like signature including Oct4 and Nanog^{13,21}, as well as Sox1 and SHH – known to be involved in adult normal neural stem cell and cancer stem cells self-renewal and maintenance^{15,22-27}. Consistent with our results, a previous report showed the importance of the miR-302-367 cluster in cell differentiation by describing its role in the promotion of mesendodermal fate specification²⁸. On the other hand, other reports described the miR-302-367 cluster as a stemness determinant in human embryonic stem cells (ESC)²⁹ and in inducible pluripotent stem cells (IPS) derived from human skin cancer cells³⁰. In those particular context, the miR-302-367 promoter was transcriptionally regulated by the stemness transcription factors Oct4, Sox2, and Nanog; therefore, its expression in the ESC compartment and during early stages of mouse development was restricted^{20,31}. In TG1 GiCs, the expression of the miR-302-367 cluster occurs concomitantly with the suppression of Oct4 and Nanog, as well as with the loss of self-renewal ability. These data suggest the existence of a mechanism distinct from that observed in pluripotent cells and particularly efficient in maintaining GiCs stem-like properties through the repression of these miRNAs. In addition, the drastic loss of the stem-like signature mediated by miR-302-367 cluster expression

suggests drastic epigenetic changes, indicating that these miRNAs might exhibit powerful regulatory potential.

Our *ex-vivo* and *in vivo* models clearly demonstrated that the miR-302-367 cluster is able to strongly suppress GiCs infiltration and tumorigenicity. This is the most important aspect of the miR-302-367 cluster activity, as tumor glial cell infiltration within the brain represents one of the main causes of the short survival time observed in GBM. In this context, we showed that the miR-302-367 cluster affects migration and clonal proliferation through a drastic inhibition of the chemokine receptor CXCR4 and its ligand SDF1. Conversely, when CXCR4 expression was restored, cell migration and proliferation were rescued. The binding of SDF1 to CXCR4 is known to trigger divergent signaling pathways such as PLC, PI3K/AKT, and MAPK, resulting in a variety of physiological responses including gene transcription, motility, survival, and proliferation³². Numerous studies reported that CXCR4 plays a role in proliferation and motility, thereby contributing to the development of highly malignant human gliomas and to tumor aggressiveness. In addition, CXCR4 expression strongly correlates with poor survival^{16,17,33}. In glioma cancer stem cells the network composed of SHH-GLI-NANOG proteins represents another important pathway involved in the regulation of proliferation, self-renewal, and expression of stemness genes^{13,15,18,19}. SHH-GLI signaling acts through positive regulators of proliferation such as the PBK/TOPK protein – a PDZ-binding kinase involved in mitosis³⁴, known to promote growth through the phosphorylation of histone H3 at Ser10^{35,36}. Here, we demonstrated that impairment of CXCR4 function leads to the drastic repression of hedgehog signaling, therefore compromising NANOG and PBK/TOPK expression and histone H3 phosphorylation at Ser10, eventually causing loss of clonal proliferation. The significant rescue of clonal proliferation mediated by exogenous recombinant SHH protein, confirms the involvement of the CXCR4 pathway in the positive regulation of the SHH-GLI1-NANOG network, and therefore its contribution in cellular self-renewal. These results emphasize the potential of CXCR4 functional inhibition as a therapeutic approach for GBM. In fact, CXCR4 inhibition would prevent tumor regrowth by inhibiting vasculogenesis³⁷ while affecting GiCs stem-like and tumorigenic properties. In a context where novel strategies for GBM treatment are much needed, the miR-302-367 cluster appears therefore to be a promising therapeutic target, as it strongly downregulates the CXCR4 pathway. The inhibition of the CXCR4 pathway is sufficient to trigger a cascade of inhibitory events that leads to the suppression of the SHH-GLI1-NANOG network, resulting in the blockade of cell infiltration and suppression of GiCs self-renewal and stem-like signature. Our data demonstrate that the miR-302-367 cluster is

not only able to inhibit the CXCR4 pathway, but it may also directly repress the cell cycle machinery by strongly inhibiting positive regulators such as E2F1, CyA and CyD1, which were already described as its putative targets²⁰. Thus, the miR-302-367 cluster not only affects GiCs stem-like and infiltrative properties, but also specifically inhibits the cell cycle machinery. The capacity of affecting different pathways involved in the promotion of cell proliferation diminishes the likelihood of cell adaptation and compensatory mechanisms, and therefore makes the miR-302-367 cluster an even more attractive therapeutic target.

In conclusion, we identified a mechanism orchestrated by the miR-302-367 cluster able to compromise GiCs stem-like and tumorigenic properties by promoting a cascade of inhibitory events – from CXCR4 inhibition to the suppression of the SHH-GLI1-NANOG network. Therefore, the miR-302-367 cluster may be a candidate target for novel therapeutic approaches aimed at attacking glioma-initiating cells.

Materials and methods

Reagents and antibodies

Cell culture reagents, pENTR cloning kit (catalog number K2400-20), LR Clonase II (catalog number 11791-020), Superscript II reverse transcriptase (catalog number 18064-014), and Trizol were purchased from Invitrogen. Foetal calf serum was from Hyclone. Hoechst 33342, U0126, TWS119, anti-B3Tubulin antibody (catalog number CBL412-diluted 1/100°) were purchased from Sigma. Anti-SHH (catalog number sc1194-diluted 1/50°) and anti-Oct4 (catalog number sc9081-diluted 1/50°) antibodies were purchased from Santa-Cruz biotechnology (tebu-bio, Leperrey en Yvelinne). Anti-Nanog (catalog number AF1997-5ug/mL), anti-CXCR4 blocking antibody (catalog number MAB170-diluted 1/100°), anti-CXCR4 (catalog number MAB 173), and anti-Olig2 (catalog number AF2418, 10ug/mL) antibodies were from R&D Systems. The CXCR4 chemical inhibitor AMD3100 (catalog number A5602) was purchased from Sigma Aldrich. Anti-GFAP (catalog number 2203PGF-1/200°) antibody was purchased from AbCys. Anti-CA (NCL-Cyclin A-diluted 1/250°) was from Novocastra. Anti-NeuN (MAB377-diluted 1/150°) was from Chemicon (Chemicon International, Temecula, CA). Anti-PKB (ab59327-diluted 1/100°) and anti-histone H3Ser10 (catalog number Ab 5176) were purchased from Abcam. Anti-species secondary antibodies coupled to Alexa 488 (diluted 1/500°) or Alexa 546 (diluted 1/500°) were purchased from Alexa. Gel/mount was purchased from Biomedica. Taqman Reverse transcription microRNA kit (catalog number 4366596), Universal Taqman PCR Master Mix, TLDA array, and

Taqman probes were purchased from Applied Biosystems. Enhanced chemiluminescence detection reagent was from Biorad.

Cell culture

The GiCs primary cell lines TG1, TG6, GB1, and #1056 were isolated from human glioblastoma¹⁴. When kept as self-renewing GiCs, neurospheres were grown in NS34+ medium containing EGF and bFGF (DMEM-F12 1/1, Glutamine 10 mM, Hepes 10 mM, Sodium bicarbonate 0,025%, N2, G5, B27). The medium for cell differentiation (MFCS) was composed of DMEM-F12, Glutamine 10 mM, Hepes 10 mM, Sodium bicarbonate 0,025%, and FCS 0.5%. In differentiation experiments, the neurospheres were dissociated and 500,000 single cells were cultured in MFCS. When necessary, the cells were incubated in NS34-minimum medium depleted of EGF and bFGF (DMEM-F12 1/1, Glutamine 10 mM, Hepes 10 mM, Sodium bicarbonate 0,025%). When indicated, the cells were treated with anti-CXCR4 antibody (1-10µg/ml) or AMD3100 (10-100 nM).

Plasmid constructs and stable cell lines

The miR-302-367 cluster was amplified from genomic DNA by PCR (Forward primer: GGCTGAAGTCCCTGCCTTTTACCC; Reverse primer: TGGCTTAACAATCCATCACCATTGC) and cloned into a pENTR commercial vector (Invitrogen, life technology). Subcloning in the 2K7 blasticidin lentiviral vector (2K7BSD) was realized by recombination in the presence of LR clonase II. Lentiviral particles were produced transfecting the 293T cell line with the 2K7BSD-Cluster mir302 or 2K7BSD-shLuc constructs along with the packaging vectors. After lentiviral infection, cell lines stably expressing the miR-302-367 cluster (TG1cluster 302 and TG6 cluster 302#1) or the control shLuc (TG1 Ctrl and TG6 Ctrl) were selected in appropriate Blasticidin NBE medium (1µg/mL) for at least 15 days. Two stable cell lines were developed from independent viral productions/infections and exhibited identical behaviors. Cells stably expressing the Red Fluorescent Protein (RFP) were obtained after 2K7BSD-RFP lentiviral particles infection. To restore CXCR4 expression, TG1 Cluster 302 and TG6 Cluster 302#1 cells were transduced with a commercially available CXCR4 lentivirus coding for a construct lacking the 3'UTR of the gene.

Immunofluorescence

Cells were grown on polylysine coated glass slides in NBE, MFCS, or TG1-cluster conditioned medium. At indicated time points, cells were washed twice with ice cold PBS, fixed with methanol 5min at -20°C , and washed again. Blocking and hybridization were performed in PBS containing 10% FCS and 0.1% Triton X100 with the following primary antibodies: anti-SHH at $1/50^{\circ}$ (N19), anti-Oct4 diluted $1/50^{\circ}$ (H-134), anti-Nanog at 5 $\mu\text{g}/\text{mL}$, anti-GFAP diluted $1/250^{\circ}$, anti-Olig2 at 10 $\mu\text{g}/\text{mL}$, anti-B3tubulin diluted $1/100^{\circ}$, anti-CyA ($1/250^{\circ}$), anti-PBK (diluted $1/150^{\circ}$), anti-CXCR4 (diluted $1/100^{\circ}$), or anti-NeuN (diluted $1/100^{\circ}$). After one hour of incubation at room temperature, cells were washed 3 times with PBS and stained 30 min at room temperature with species-specific fluorophore-coupled antibodies. At the same time, nuclei were stained with Hoechst 33342 (1 $\mu\text{g}/\text{mL}$). The slides were washed twice with PBS, once with distilled water, and finally mounted with gel/mount. Immunofluorescence and transmission light pictures were taken with a Nikon eclipse Ti microscope.

Clonogenic assay

Neurospheres were dissociated by gently pipeting up and down to obtain a single cell suspension. Ten cells were seeded in each well of 96 wells plates in NBE/NS34+ medium containing, when indicated, anti-CXCR4 blocking antibody. After one month, each well was examined and the number of neurospheres/well was counted. Experiments were repeated three independent times.

Quantitative real-time RT-PCR

RNA was extracted using Trizol reagent (Invitrogen, Invitrogen SARL BP 9695613 Cergy Pontoise Cedex). MicroRNA and mRNA expression levels were quantified by two step real-time RT-PCR. Reverse transcription steps were performed with Superscript II reverse transcriptase and Taqman Reverse transcription microRNA kit for mRNA and miRNA, respectively, following the manufacturer's instructions. Real time PCRs were performed using universal Taqman PCR Master Mix. U54 expression was used as internal control to determine the relative expression of each gene. Fold changes were estimated using the $\Delta\Delta\text{CT}$ method. miRNA screening was performed using TAQMAN TLDA arrays (Applied Biosystems), following the manufacturer's instructions. The results have been normalized using expression of small nucleolar RNA, according to the manufacturer's protocol. The fold changes were calculated and normalized using the $\Delta\Delta\text{CT}$ method.

Orthotopic xenografts

TG1 Ctrl and TG1 Cluster 302 cells (2×10^5) were resuspended in 5 μ l of Hanks balanced salt solution (Invitrogen) and stereotactically implanted unilaterally into the striatum of male NOD.CB17-Prkdcscid/NCrHsd mice, (Harlan). The cells stably expressed a luciferase reporter gene, which allowed tumor detection in living animals. Two groups of 5 mice were injected. Cell survival and tumor growth were monitored and quantified in the living animals up to 30 days using the IVIS Lumina II system (Caliper Life Sciences).

Organotypic mouse brain slice (MBS) culture

Brains were dissected from new-born mice, embedded in 4% agar-agar Artificial CerebroSpinal Fluid (NaCl 124 mM, KCl 3 mM, NaHCO₃ 26mM, CaCl₂ 2 mM, MgSO₄ 1mM, KH₂PO₄ 1.25 mM, Glucose 10mM), and cut in slices of 400 μ m thickness using a vibratome. The slices were placed on a Millicell-CM (0.4 μ m) culture plate, inserted and maintained under air-liquid interface conditions for more than three weeks without any necrosis.

Paraffin Embedding

Organotypic cultures (brain slides) or tissues were fixed with 4% paraformaldehyde for 20 min at room temperature, then washed with PBS. Samples were subsequently dehydrated with the following sequence of incubations: ethanol 70% 15 min, twice; ethanol 90% 15 min; ethanol 95% 15 min; ethanol 100% 5 min, thrice; Rotoclear 5min.

Ex vivo tumorigenesis assay

About 10 neurospheres from TG1 Ctrl and TG1 Cluster 302 cells stably expressing the red fluorescent protein were seeded at the top surface of the MBS and cultured under air-liquid interface conditions for 3 weeks. Cell infiltration and growth was visualized by tracking the red fluorescent protein signal using a Nikon eclipse Ti microscope. When indicated, a drop of medium containing anti-CXCR4 blocking antibody or the chemical inhibitor AMD3100 was added to the brain slice every 4 days.

Acknowledgements

This work was supported by grants from Association pour la Recherche sur le Cancer (subvention 3161), Association Sauvons Laura, Agence Nationale pour la Recherche (ANR

jeune chercheur), INSERM, UNSA, OSEO/VALORPACA. We thank Dr Rassoulzadegan's lab (Inserm U636, F-06108 Nice, France) for their contribution in our organotypic culture model of mouse brain.

References

1. Stupp, R, Mason, WP, van den Bent, MJ, Weller, M, Fisher, B, Taphoorn, MJ et al., (2005) Radiotherapy plus concomitant and adjuvant temozolomide for glioblastoma. *N Engl J Med* 352: 987-96.
2. Wen, PY and Kesari, S, (2008) Malignant gliomas in adults. *N Engl J Med* 359: 492-507.
3. Shannon, RP, Sayre, JW and Sayre, JJ, (2005) Patterns of care for adults with malignant glioma. *Jama* 293: 2469-70; author reply 2470.
4. Hegi, ME, Diserens, AC, Godard, S, Dietrich, PY, Regli, L, Ostermann, S et al., (2004) Clinical trial substantiates the predictive value of O-6-methylguanine-DNA methyltransferase promoter methylation in glioblastoma patients treated with temozolomide. *Clin Cancer Res* 10: 1871-4.
5. Germano, I, Swiss, V and Casaccia, P, (2010) Primary brain tumors, neural stem cell, and brain tumor cancer cells: Where is the link? *Neuropharmacology*.
6. Passegue, E, Jamieson, CH, Ailles, LE and Weissman, IL, (2003) Normal and leukemic hematopoiesis: are leukemias a stem cell disorder or a reacquisition of stem cell characteristics? *Proc Natl Acad Sci U S A* 100 Suppl 1: 11842-9.
7. Smalley, M and Ashworth, A, (2003) Stem cells and breast cancer: A field in transit. *Nat Rev Cancer* 3: 832-44.
8. Wu, W, Patents related to cancer stem cell research. *Recent Pat DNA Gene Seq* 4: 40-5.
9. Visvader, JE and Lindeman, GJ, (2008) Cancer stem cells in solid tumours: accumulating evidence and unresolved questions. *Nat Rev Cancer* 8: 755-68.
10. Piccirillo, SG and Vescovi, AL, (2006) Bone morphogenetic proteins regulate tumorigenicity in human glioblastoma stem cells. *Ernst Schering Found Symp Proc* 5: 59-81.
11. Rao, M, (2004) Conserved and divergent paths that regulate self-renewal in mouse and human embryonic stem cells. *Dev Biol* 275: 269-86.
12. Wang, Y, Medvid, R, Melton, C, Jaenisch, R and Blelloch, R, (2007) DGCR8 is essential for microRNA biogenesis and silencing of embryonic stem cell self-renewal. *Nat Genet* 39: 380-5.
13. Zbinden, M, Duquet, A, Lorente-Trigos, A, Ngwabyt, SN, Borges, I and Ruiz, IAA, (2010) NANOG regulates glioma stem cells and is essential in vivo acting in a cross-functional network with GLI1 and p53. *Embo J*.
14. Patru, C, Romao, L, Varlet, P, Coulombel, L, Raponi, E, Cadusseau, J et al., (2010) CD133, CD15/SSEA-1, CD34 or side populations do not resume tumor-initiating properties of long-term cultured cancer stem cells from human malignant glioma neuronal tumors. *BMC Cancer* 10: 66.
15. Clement, V, Sanchez, P, de Tribolet, N, Radovanovic, I and Ruiz i Altaba, A, (2007) HEDGEHOG-GLI1 signaling regulates human glioma growth, cancer stem cell self-renewal, and tumorigenicity. *Curr Biol* 17: 165-72.
16. Ehteshami, M, Stevenson, CB and Thompson, RC, (2008) Preferential expression of

- chemokine receptor CXCR4 by highly malignant human gliomas and its association with poor patient survival. *Neurosurgery* 63: E820; author reply E820.
17. do Carmo, A, Patricio, I, Cruz, MT, Carvalheiro, H, Oliveira, CR and Lopes, MC, (2010) CXCL12/CXCR4 promotes motility and proliferation of glioma cells. *Cancer Biol Ther* 9.
 18. Shi, Y, Sun, G, Zhao, C and Stewart, R, (2008) Neural stem cell self-renewal. *Crit Rev Oncol Hematol* 65: 43-53.
 19. Lai, K, Kaspar, BK, Gage, FH and Schaffer, DV, (2003) Sonic hedgehog regulates adult neural progenitor proliferation in vitro and in vivo. *Nat Neurosci* 6: 21-7.
 20. Card, DA, Hebbar, PB, Li, L, Trotter, KW, Komatsu, Y, Mishina, Y et al., (2008) Oct4/Sox2-regulated miR-302 targets cyclin D1 in human embryonic stem cells. *Mol Cell Biol* 28: 6426-38.
 21. Ben-Porath, I, Thomson, MW, Carey, VJ, Ge, R, Bell, GW, Regev, A et al., (2008) An embryonic stem cell-like gene expression signature in poorly differentiated aggressive human tumors. *Nat Genet* 40: 499-507.
 22. Alcock, J and Sottile, V, (2009) Dynamic distribution and stem cell characteristics of Sox1-expressing cells in the cerebellar cortex. *Cell Res* 19: 1324-33.
 23. Wegner, M and Stolt, CC, (2005) From stem cells to neurons and glia: a Soxist's view of neural development. *Trends Neurosci* 28: 583-8.
 24. Palma, V, Lim, DA, Dahmane, N, Sanchez, P, Brionne, TC, Herzberg, CD et al., (2005) Sonic hedgehog controls stem cell behavior in the postnatal and adult brain. *Development* 132: 335-44.
 25. Elkouris, M, Balaskas, N, Poulou, M, Politis, PK, Panayiotou, E, Malas, S et al., Sox1 Maintains the Undifferentiated State of Cortical Neural Progenitor Cells Via the Suppression of Prox1-Mediated Cell Cycle Exit and Neurogenesis. *Stem Cells*.
 26. Salcido, CD, Larochelle, A, Taylor, BJ, Dunbar, CE and Varticovski, L, Molecular characterisation of side population cells with cancer stem cell-like characteristics in small-cell lung cancer. *Br J Cancer* 102: 1636-44.
 27. Wright, MH, Calcagno, AM, Salcido, CD, Carlson, MD, Ambudkar, SV and Varticovski, L, (2008) Brca1 breast tumors contain distinct CD44+/CD24- and CD133+ cells with cancer stem cell characteristics. *Breast Cancer Res* 10: R10.
 28. Rosa, A, Spagnoli, FM and Brivanlou, AH, (2009) The miR-430/427/302 family controls mesendodermal fate specification via species-specific target selection. *Dev Cell* 16: 517-27.
 29. Barroso-del Jesus, A, Lucena-Aguilar, G and Menendez, P, (2009) The miR-302-367 cluster as a potential stemness regulator in ESCs. *Cell Cycle* 8: 394-8.
 30. Lin, SL, Chang, DC, Chang-Lin, S, Lin, CH, Wu, DT, Chen, DT et al., (2008) Mir-302 reprograms human skin cancer cells into a pluripotent ES-cell-like state. *Rna* 14: 2115-24.
 31. Barroso-delJesus, A, Romero-Lopez, C, Lucena-Aguilar, G, Melen, GJ, Sanchez, L, Ligerio, G et al., (2008) Embryonic stem cell-specific miR302-367 cluster: human gene structure and functional characterization of its core promoter. *Mol Cell Biol* 28: 6609-19.
 32. Teicher, BA and Fricker, SP, (2010) CXCL12 (SDF-1)/CXCR4 pathway in cancer. *Clin Cancer Res* 16: 2927-31.
 33. Ehtesham, M, Mapara, KY, Stevenson, CB and Thompson, RC, (2009) CXCR4 mediates the proliferation of glioblastoma progenitor cells. *Cancer Lett* 274: 305-12.
 34. Dougherty, JD, Garcia, AD, Nakano, I, Livingstone, M, Norris, B, Polakiewicz, R et al., (2005) PBK/TOPK, a proliferating neural progenitor-specific mitogen-activated protein kinase kinase. *J Neurosci* 25: 10773-85.

35. Park, JH, Lin, ML, Nishidate, T, Nakamura, Y and Katagiri, T, (2006) PDZ-binding kinase/T-LAK cell-originated protein kinase, a putative cancer/testis antigen with an oncogenic activity in breast cancer. *Cancer Res* 66: 9186-95.
36. Hans, F and Dimitrov, S, (2001) Histone H3 phosphorylation and cell division. *Oncogene* 20: 3021-7.
37. Kioi, M, Vogel, H, Schultz, G, Hoffman, RM, Harsh, GR and Brown, JM, Inhibition of vasculogenesis, but not angiogenesis, prevents the recurrence of glioblastoma after irradiation in mice. *J Clin Invest* 120: 694-705.

Figure legends

Figure 1: **The miR-302-367 cluster contributes to serum-mediated suppression of GICs stemness.** (A) Immunofluorescence and (B, upper panel) quantitative real-time PCR (QPCR) were used to detect SHH and the glial markers GFAP and OLIG2 expression in self-renewing or serum-differentiated TG1 cells. The lower panel of (B) represents the clonal efficiency of self-renewing and serum-treated TG1 cells. (C) Measurement of miRNAs over-expressed after 4 days of serum-mediated differentiation, by Taqman Low Density Array (TLDA). The circle highlights the miR-302-367 cluster. (D) QPCR analysis of the miR-302-367 cluster at different time points (1, 2, 3, 8, and 15 days) of serum-mediated differentiation. Self-renewing TG1 cells were cultured either in their defined medium or in 0.5% serum to induce differentiation. At each time point, total RNA was extracted and expression of miR-302a, b, c, d, and 367 was determined using Taqman probe as described in the Materials and Methods section. (E) Anti-miR-302a, anti-miR-302b, anti-miR-367 or (F) a pool of the three anti-miRs were used to transiently transfect TG1 cells to determine the importance of individual or simultaneous functional inhibition of these specific miR in serum-mediated differentiation (Diff). Four days following transfection, SHH, GFAP, and OLIG2 expression were assessed by QPCR. siLUC was used as control.

Figure 2: **miR-302-367 cluster expression promotes a phenotype similar to that of differentiated cells.** Stable primary cell lines TG1 (A) and TG6 (B) expressing the miR-302-367 cluster (TG1 Cluster 302 and TG6 Cluster 302#1) or a non-relevant small non-coding RNA construct (TG1 Ctrl and TG6 Ctrl) were generated. Relative expression of each miRNA of the miR-302-367 cluster was assessed by QPCR using taqman probes in TG1 Cluster 302, TG2 Cluster 302#1 and their respective control cells (lower panels). Upon EGF and bFGF removal, only TG1 Cluster 302 and TG2 Cluster 302#1 cells became adherent and exhibited a morphology typical of differentiated cell (pictures on the right), while TG1 and TG6 Ctrl cells

remained unchanged. (C) Expression of GFAP and SHH, in TG Cluster 302 cells compared to TG Ctrl cells was assessed by QPCR after 4 days of culture in bFGF and EGF depleted medium. Error bars are derived from 3 independent experiments.

Figure 3: Stable miR-302-367 cluster expression induces loss of stemness and upregulation of glial markers. (A) Expression of stemness markers (SHH, Oct4, Nanog, and Sox1) was evaluated by immunofluorescence in TG1 Ctrl (upper panels) or TG1 Cluster 302 cells (lower panels). Cells were cultured in growing medium containing EGF and bFGF (NS34+), which are required for GiCs proliferation and self-renewal. (B) Expression of glioneuronal markers (GFAP and NeuN) was evaluated by immunofluorescence in TG1 Cluster 302 cells cultured either in NS34+ (left panel) or in medium depleted of EGF and bFGF (NS34-) (day 1, middle panel; day 4 right panel). Nuclei were stained with DAPI.

Figure 4: The miR-302-367 cluster inhibits clonogenicity and infiltrative properties of TG1 GiCs. (A) TG1 Ctrl and TG1 Cluster 302 cells were seeded at a density of 10 cells/well in a 96 wells plate and allowed to grow. After 1 month, the neurospheres were counted; 10 neurospheres/well corresponded to a clonal efficiency of 100%. Error bars are derived from 3 independent experiments. Statistical analysis was performed using Student's t-test: **** corresponds to a P-value of $4.4 \cdot 10^{-18}$ and indicates a highly significant difference between the clonal efficiency of TG1 Ctrl and TG1 Cluster 302 cells. The pictures below the plot show the size difference between the neurospheres formed by TG1 Ctrl cells and those formed by TG1 Cluster 302 cells. (B) The DNA content of TG1 Ctrl and TG1 Cluster 302 cells was labeled with propidium iodide. Cell cycle profile was assessed by FACS. (C) 80,000 TG1 Ctrl (solid line) and TG1 Cluster 302 (dashed line) cells were seeded in a 35mm diameter culture dish. The cells were then counted at each indicated time point. Error bars are derived from 3 independent experiments. (D) TG1 Ctrl and TG1 Cluster 302 cells stably expressing the red fluorescent protein were seeded on a nylon filter under air-liquid interface conditions as described in the Materials and Methods and allowed to grow. After 1 month, the filter was embedded in paraffin and sliced. The red fluorescent protein showed the growth and development of a tumor-like tissue *in vitro* only in the case of TG1 Ctrl cells. (E) TG1 Ctrl and TG1 Cluster 302 cells stably expressing the red fluorescent protein, were seeded on the top surface of an organotypic brain slice culture of mouse brain, as described in the Materials and Methods section. Block 1 and 2 represent two independent organotypic brain slice cultures. The right panel shows phase contrast picture of red fluorescent TG1 Ctrl and TG1

Cluster 302 cells seeded on the top surface of the mouse brain slice (Block 2). After 1 month, each organotypic culture was embedded in paraffin and sliced. Cell infiltration and growth within the neural host tissue was visualized by tracking the red fluorescent protein. Dashed lines mark the neural tissue boundaries. The histogram in the middle panel represents a measurement of the fluorescence intensity quantified using the Image J software. The values were compared to the background fluorescence measured in the same conditions in unseeded mouse brain slices.

Figure 5: The miR-302-367 cluster inhibits tumor development *in vivo*. TG1 Ctrl and TG1 Cluster 302 cells were orthotopically implanted into the striatum of male NOD.CB17-Prkdcscid/NCrHsd mice. Tumors were visualized (A) and their growth was quantified (B) as described in the Materials and Methods section.

Figure 6: The miR-302-367 cluster promotes CXCR4 functional inhibition. (A) In silico analysis revealing the position of putative miR-302-367 cluster interactions on CXCR4 and SDF1 3'UTR. (B) TG1 cells were transiently transfected either with the miR-302-367 cluster construct (Cluster 302) or with a non-relevant small non-coding RNA as control (Ctrl). Four days after transfection, total RNA was extracted and the level of expression of CXCR4 and SDF1 mRNA was assessed by QPCR. Results are represented as relative expression compared with the Ctrl. (C) TG1 Cluster 302 cells were transfected either with a non-relevant siRNA siLUC or with a pool of anti-miR specific for miR-302a and 302b (clear miR-302a/b). Total RNA was extracted and the level of expression of CXCR4 was assessed by QPCR. The results are expressed as relative expression compared with siLUC transfected TG1 Ctrl cells. Error bars are derived from 3 independent experiments. (D) 293T cells were transiently transfected with a construct expressing the luciferase gene fused to the WT CXCR4 3'UTR or lacking the miR-302 binding site along with miR-302a or the non-relevant miR-23. (E) CXCR4 protein expression was assessed by immunofluorescence in both TG1 Ctrl and TG1 Cluster 302 cells. Nuclei were stained with DAPI. (F) Boyden chambers assays were performed using TG1 Ctrl and TG1 Cluster 302 cells in the presence or absence of the CXCR4 ligand SDF1.

Figure 7: CXCR4 functional inhibition suppresses TG1 infiltration within a cerebral tissue. TG1 Ctrl cells were pre-incubated or not with the CXCR4 inhibitor AMD3100 or with anti-CXCR4 blocking antibody for 24 hours. These cells, as well as TG1 Cluster 302 cells

(Cluster 302), were then seeded on the surface of a mouse brain slice. The upper panels (Surface of brain slice) show cell interactions with the surface of the brain slice. The lower panels (Paraffin sections) represent paraffin sections showing cells infiltration only in the control condition (Ctrl). Dashed lines mark the neural tissue boundaries. Block1 and 2 show the section of two different mouse brain slices. The white arrows indicate the surface on which the cells were seeded. (B) The histogram represents a measurement of the fluorescence intensity quantified using the Image J software. The values were compared to the background fluorescence measured in the same conditions in unseeded mouse brain slices.

Figure 8: CXCR4 functional inhibition impairs the SHH-GLI1-NANOG network leading to a drastic loss of clonal proliferation. (A) TG1 cells were treated with anti-CXCR4 blocking antibody (anti CXCR4) or not (Ctrl). A clonogenic assay was then performed by seeding 10 cells/well, as described in the Materials and Methods section. Ten neurospheres/well corresponded to a clonal efficiency of 100%. Error bars are derived from 3 independent experiments. Statistical analysis was performed using Student's t-test; **** corresponds to a P-value of $3.4 \cdot 10^{-13}$ and indicates a highly significant difference between the control and treated cells. (B) SHH and GLI1 mRNA expression levels were assessed by QPCR using taqman probes in cells treated with AMD3100 or anti-CXCR4 antibody, in control cells (Ctrl), and in TG1 cluster 302 cells in which CXCR4 expression was restored by a CXCR4 construct lacking the 3'UTR sequences. (C) SHH and NANOG expression at the protein level was assessed by immunofluorescence in TG1 cells treated with anti-CXCR4 or not (Ctrl) and in TG1 Cluster 302 cells. (D) SHH and NANOG expression at the protein level was assessed in TG1 Cluster 302 cells in which CXCR4 expression was restored by a CXCR4 construct lacking the 3'UTR sequences. (E) TG1 cells treated with anti-CXCR4 blocking antibody (anti CXCR4) or not (Ctrl), and TG1 cluster 302 cells were grown in the presence or absence of recombinant SHH protein. A clonogenic assay was performed by seeding 10 cells/well as described in the Materials and Methods section. Ten neurospheres/well corresponded to a clonal efficiency of 100%. Error bars are derived from 3 independent experiments. Statistical analysis was performed using Student t-test; *** corresponds to a P-value of 10^{-4} and indicates a highly significant difference between the control and treated cells. (F) Quantification of TG1 cells treated with anti-CXCR4 or not (Ctrl) and TG1 Cluster 302 cells positive for PBK/TOPK kinase or Histone H3Ser10. (G) E2F1, CyA, and CyD1 mRNA expression were assessed in TG1 cells treated or not with anti-CXCR4 and in TG1 Cluster 302 cells. Results are expressed as relative expression compared with untreated TG1

cells and TG1 Ctrl cells stably expressing a non-relevant small non-coding RNA, respectively.

Supplementary figure legends

Supplementary Figure 1: (A) Expression of the stemness markers Oct4 and Nanog was assessed by immunofluorescence in self-renewing and serum-differentiated TG1 cells. Nuclei were stained with DAPI. (B) Expression of the miR-302-367 cluster was determined by QPCR analysis after 4 days of serum-mediated differentiation using Taqman Low Density Array (TLDA). ND refers to “not detected”, CT to cycle threshold. Error bars are derived from 3 independent experiments. (C) QPCR analysis of miR-302-367 cluster expression during serum-mediated differentiation. Self-renewing TG6 cells were cultured either in their defined medium or in 0.5% serum to induce differentiation. Total RNA was extracted at different time points (1, 2, 3, 8, and 15 days), and the expression of miR-302a, b, c, d, and 367 was determined using Taqman probe as described in the Materials and Methods section. (D) Expression of miR-302-367 cluster members in two other self-renewing primary cell lines obtained from glioblastoma (GB1 and #1056).

Supplementary Figure 2: (A) TG1 cells were transfected either with the non-relevant control siLUC or with anti-miR-302a, anti-miR-302b, or anti-miR-367. The day following the transfection, the cells were treated with serum to induce differentiation. (B) An identical experimental setting was used to transfect self-renewing TG1 cells either with the control siLUC or with a pool of the three anti-miR (anti-miR-302a, anti-miR-302b, and anti-miR-367). After 3 days, miR-302a, miR-302b, and miR-367 expression levels were assessed by QPCR using taqman probes and compared to their relative expression in self-renewing TG1. Error bars are derived from 3 independent experiments.

Supplementary Figure 3: (A) Expression of stemness markers (SHH, Oct4, Nanog) was assessed by immunofluorescence in TG6 Ctrl (upper panels) and TG6 Cluster 302 (lower panels) cells cultured in growing medium containing EGF and bFGF (NS34+) – required for GiCs proliferation and self-renewal. Expression of glioneuronal markers (GFAP and NeuN) was assessed by immunofluorescence in TG6 Cluster 302#1 cells cultured in NS34+ (B) or after 4 days of culture in medium depleted of EGF and bFGF (NS34-) (C). Nuclei were stained with DAPI. (D) TG6 Ctrl and TG6 Cluster 302#1 cells were seeded at a density of 10 cells/well in a 96 wells plate and allowed to grow. After 1 month the neurospheres were

counted; 10 neurospheres/well corresponded to a clonal efficiency of 100%. Error bars are derived from 3 independent experiments. Statistical analysis was performed using Student's t-test; **** corresponds to a P-value of 10^{-14} and indicates a highly significant difference between the clonal efficiency of TG6 Ctrl and TG6 Cluster 302#1 cells. (E) TG6 Ctrl and TG6 Cluster 302#1 cells stably expressing the red fluorescent protein, were seeded on the top surface of organotypic brain slice culture of mouse brain, as described in the Materials and Methods section. After 1 month, each organotypic culture was embedded in paraffin and sliced. Cell infiltration and growth within the neural host tissue was visualized by tracking the red fluorescent protein. Dashed lines mark the neural tissue boundaries. The histogram represents a measurement of the fluorescence intensity quantified using the Image J software. The values are compared to the background fluorescence measured in the same conditions in unseeded mouse brain slices.

Supplementary Figure 4: (A) TG6 Cluster 302#1 cells were transfected either with a non-relevant siRNA siLUC or with a pool of anti-miR specific for miR-302a and 302b (clear miR-302a/b). Total RNA was extracted and CXCR4 mRNA levels were assessed by QPCR. The results are expressed as relative expression compared with siLUC transfected TG1 Ctrl cells. Error bars are derived from 3 independent experiments. (B) CXCR4 protein expression was assessed by immunofluorescence in TG6 Ctrl and TG6 Cluster 302#1 cells. Nuclei were stained with DAPI. (C) Boyden chambers assays were performed using TG6 Ctrl or TG6 Cluster 302#1 cells in the presence or absence of the CXCR4 ligand SDF1. (D) Boyden chambers assays were performed using TG6 Ctrl cells, TG6 Cluster 302#1 cells, and TG6 Cluster 302#1 cells in which CXCR4 expression was restored by a CXCR4 construct lacking the 3'UTR sequences.

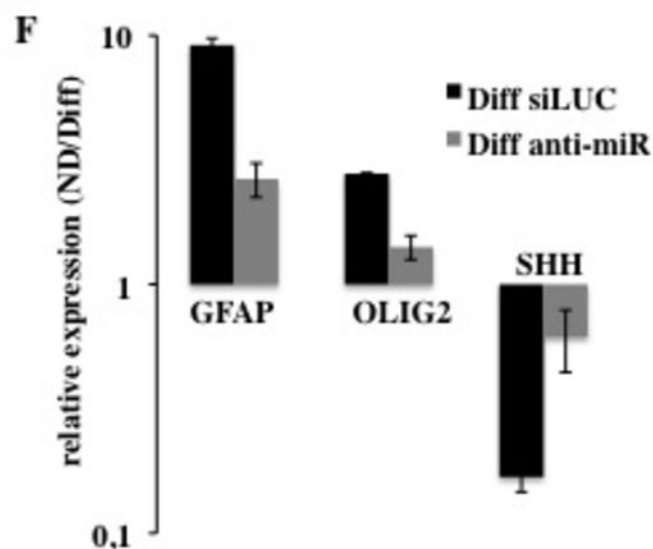
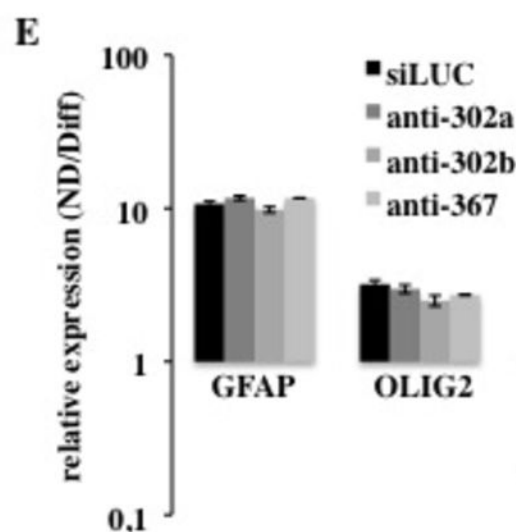
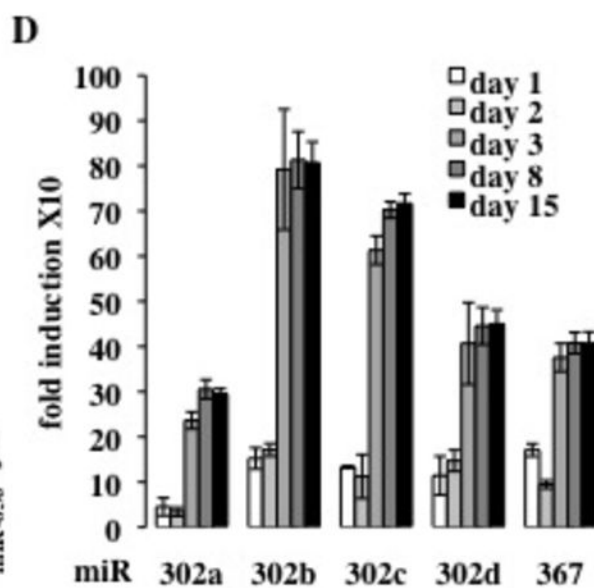
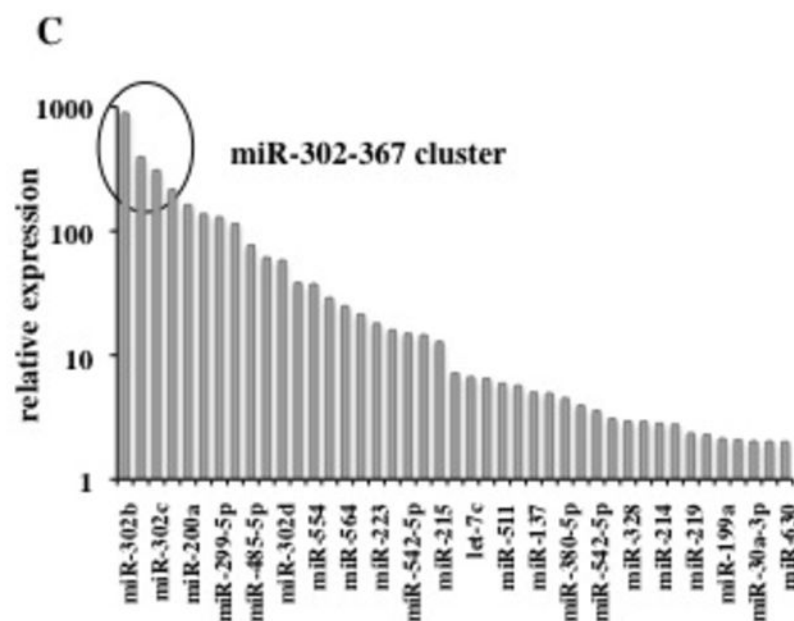
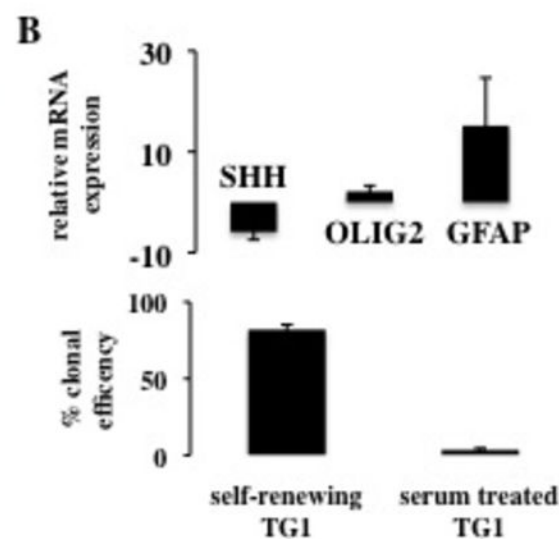
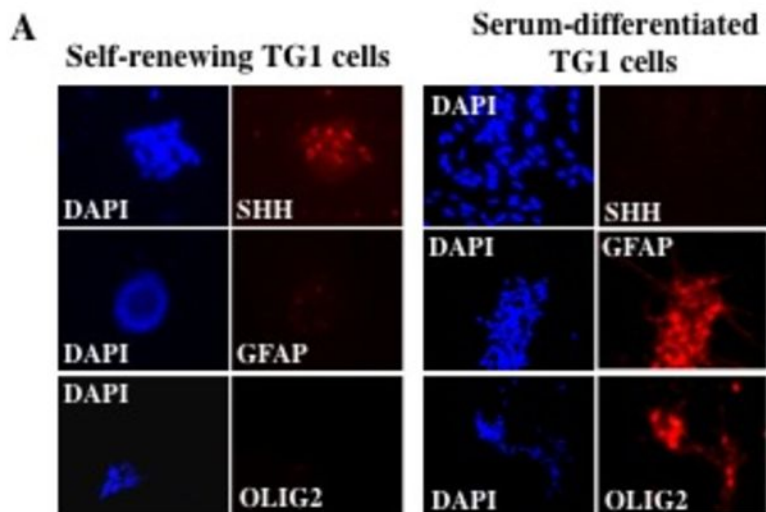
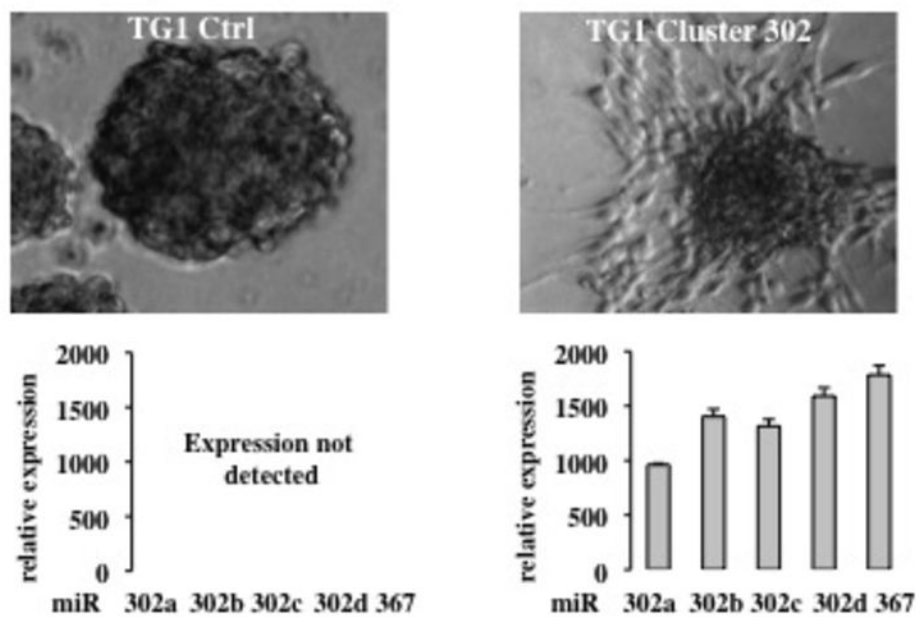


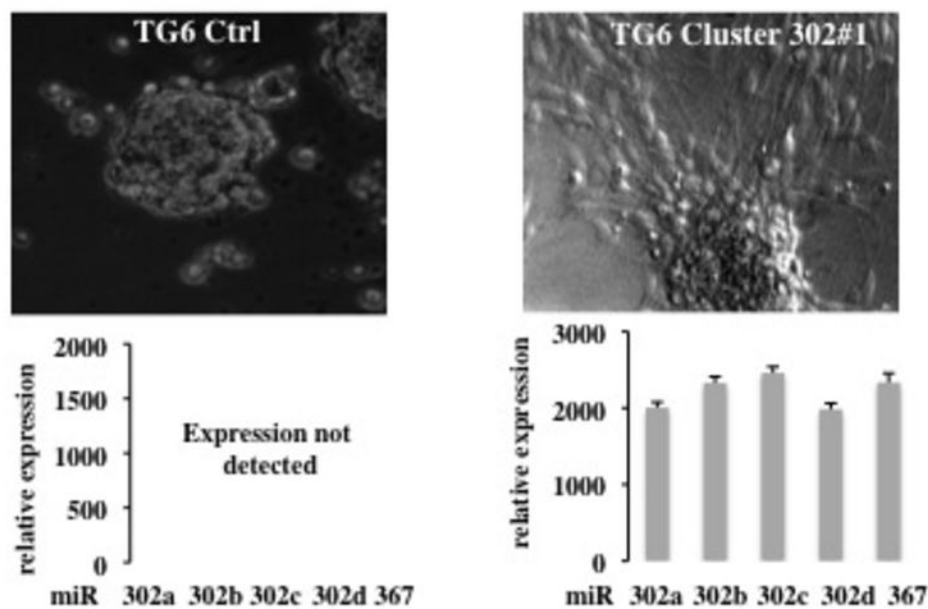
Figure 1

Stable expression

A



B



C

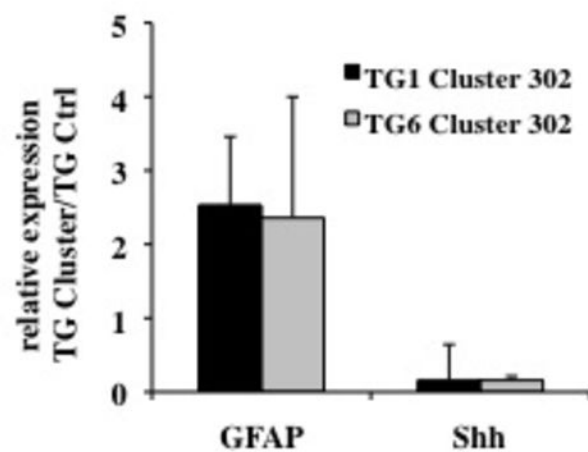
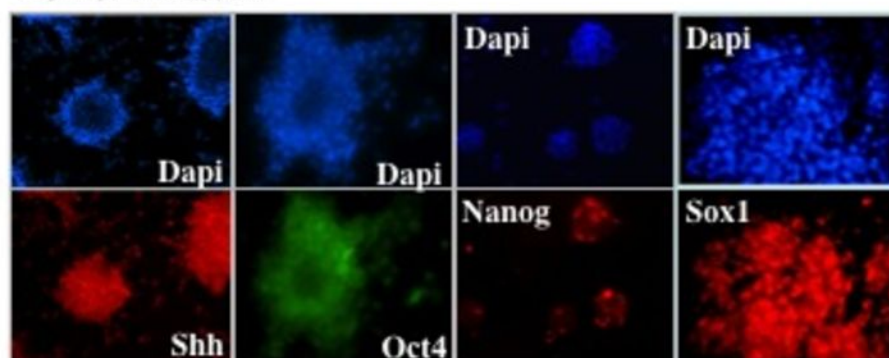


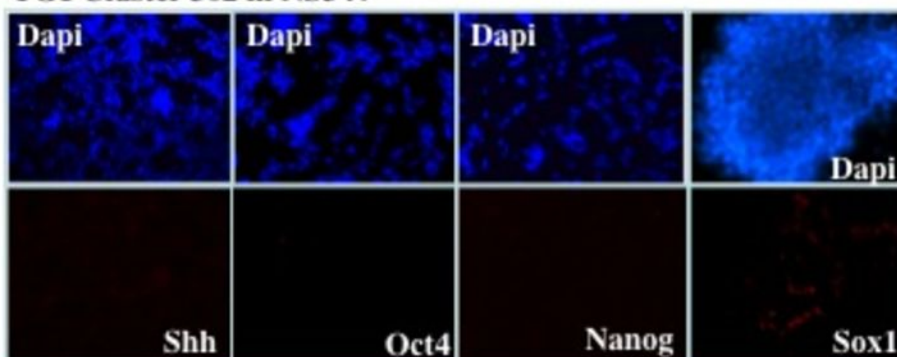
Figure 2

A

TG1 Ctl in NS34+



TG1 Cluster 302 in NS34+



B

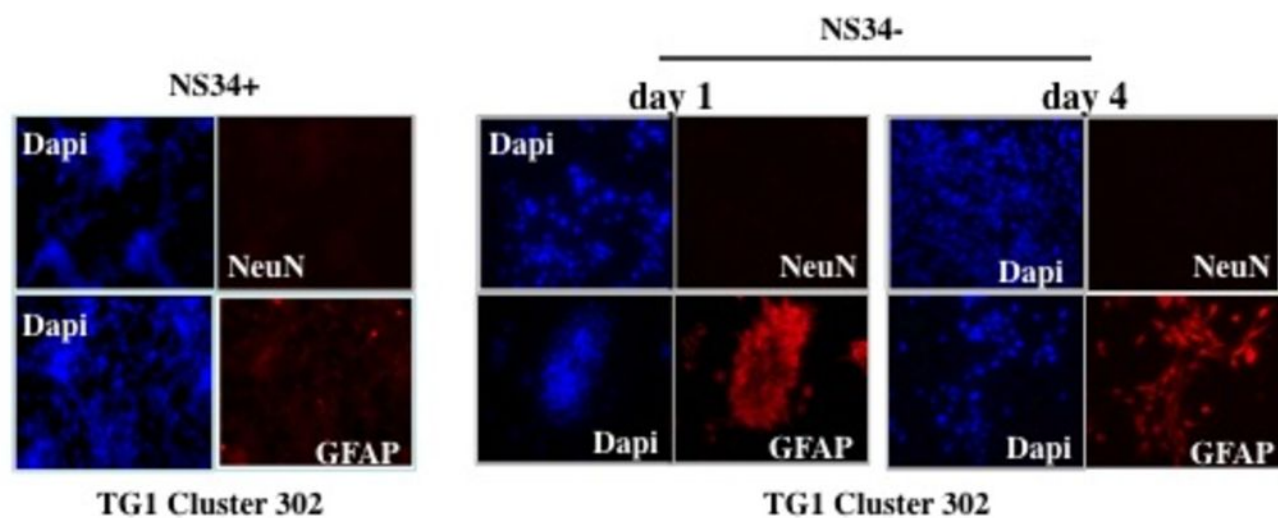


Figure 3

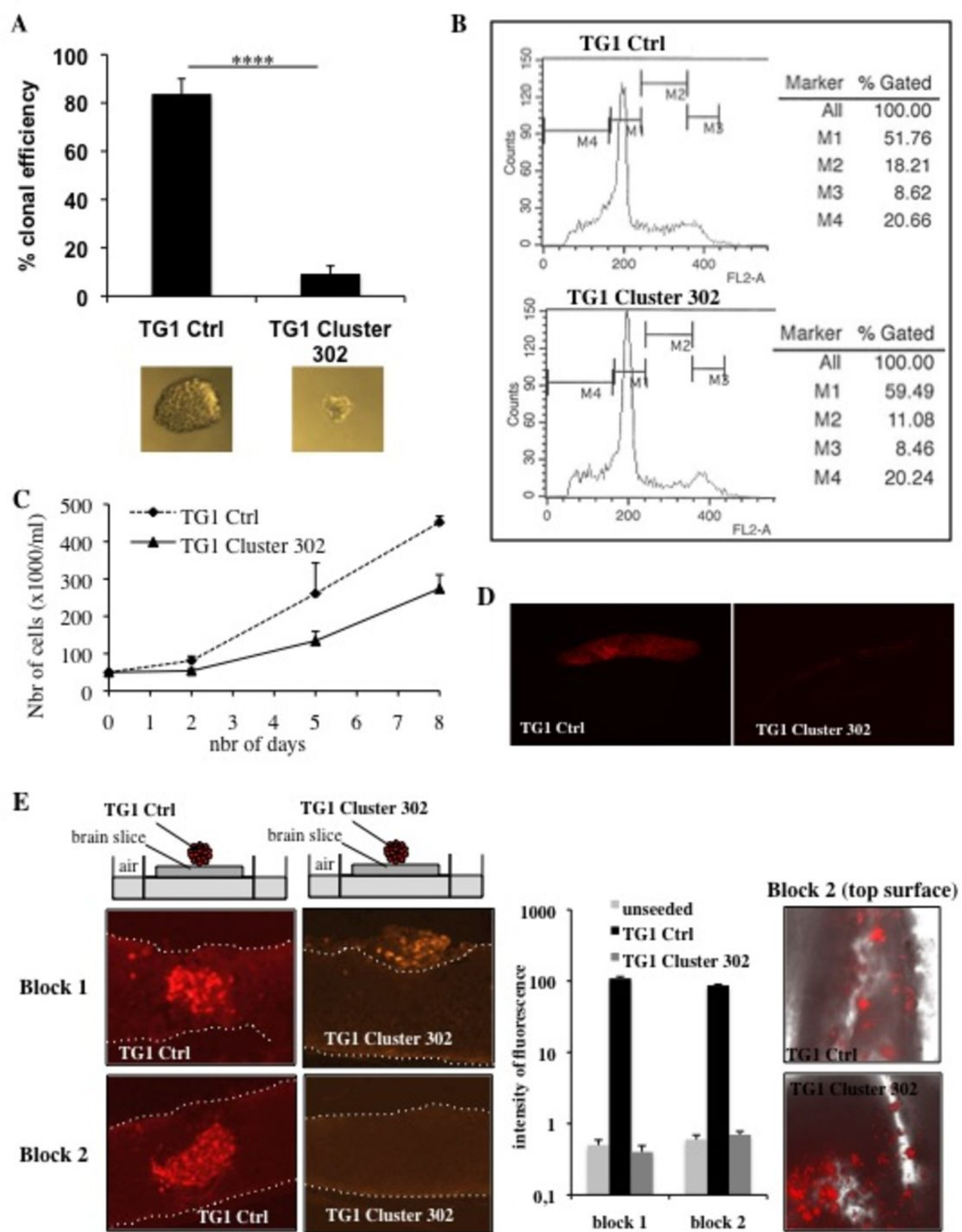


Figure 4

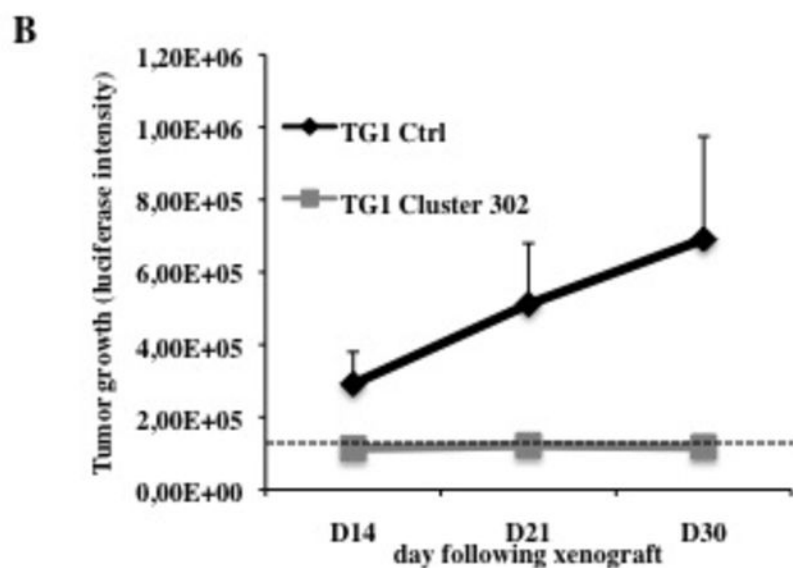
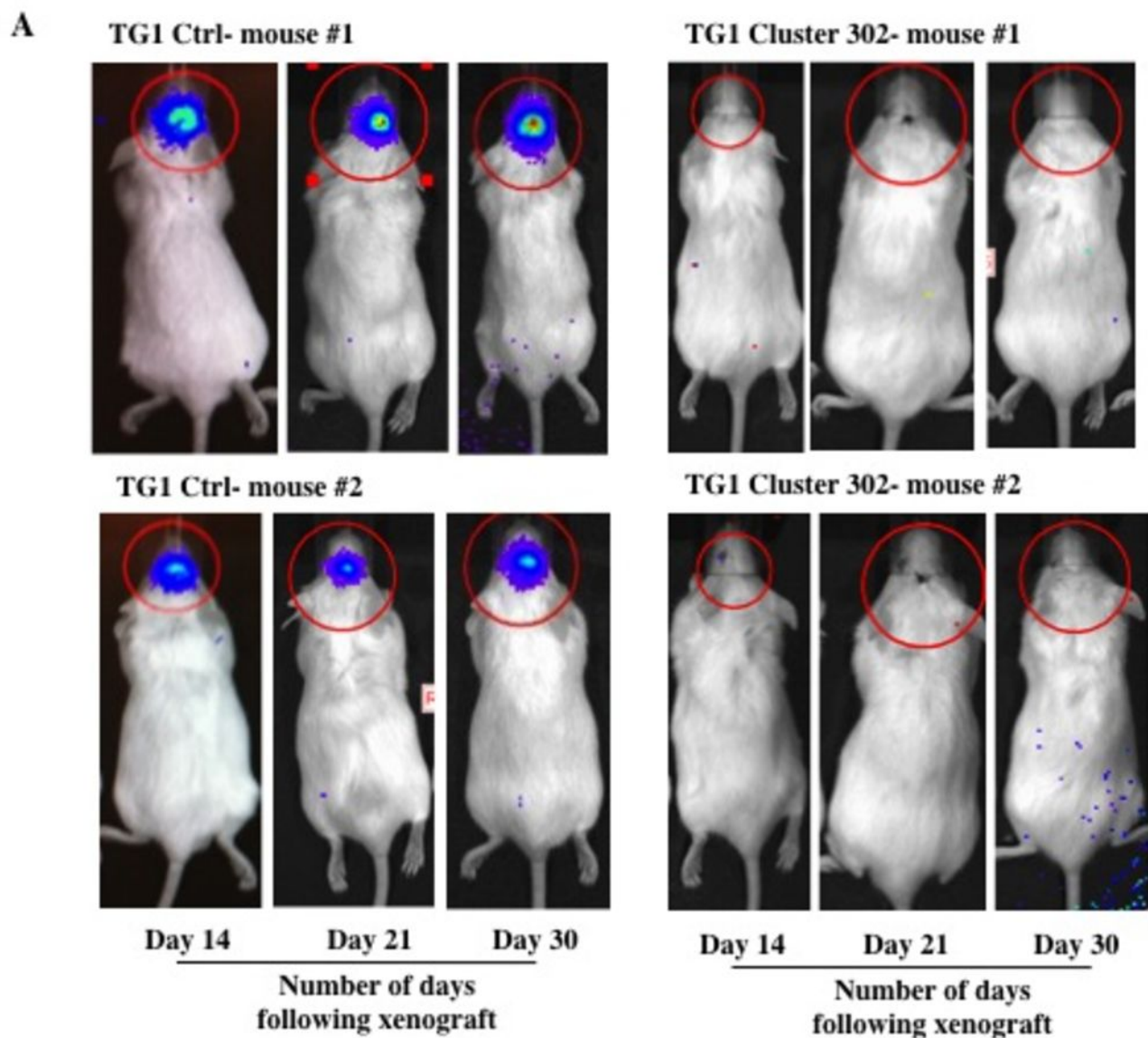
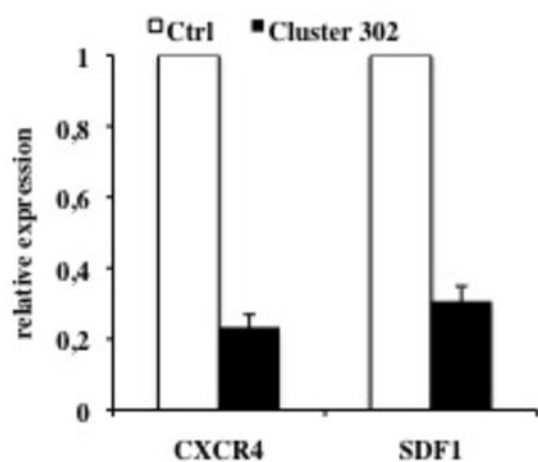
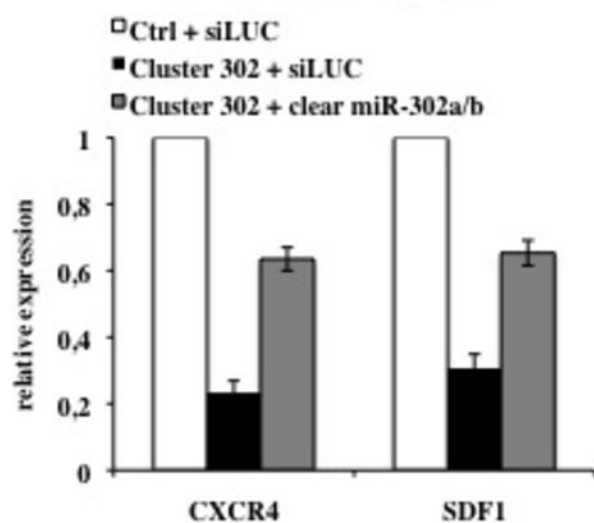
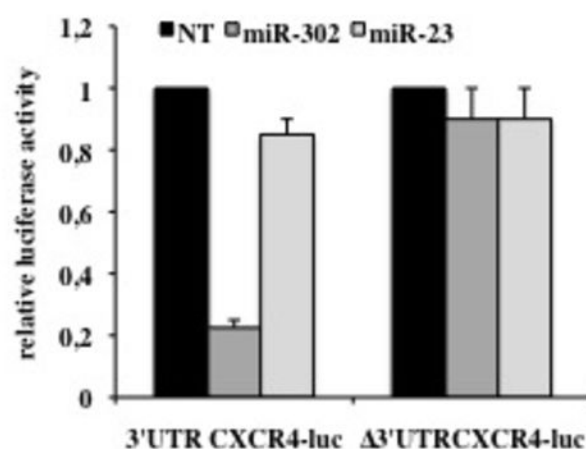
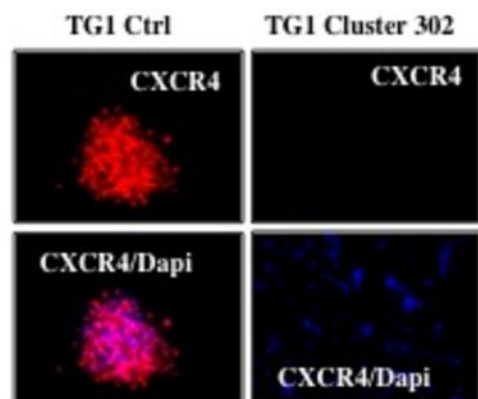
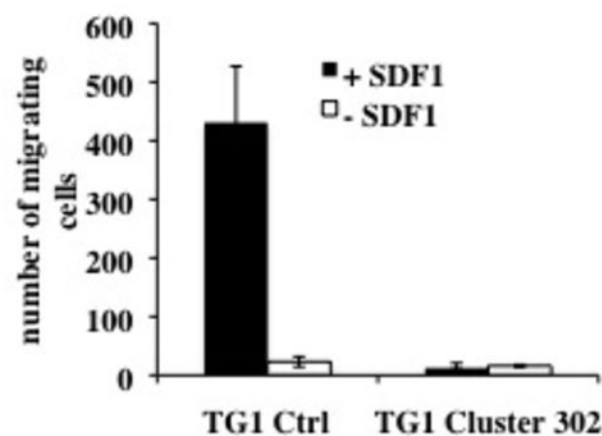


Figure 5

A

TARGETS	miR-302a	miR-302b	miR-302c	miR-302d
Seed position in CXCR4 3'UTR	392-398	392-398	392-398	392-398
Seed position in SDF1 3'UTR	159-167	159-167 363-369	159-167 290-296	159-167

B miR-302-367 transient expression**C miR-302-367 stable expression****D****E****F****Figure 6**

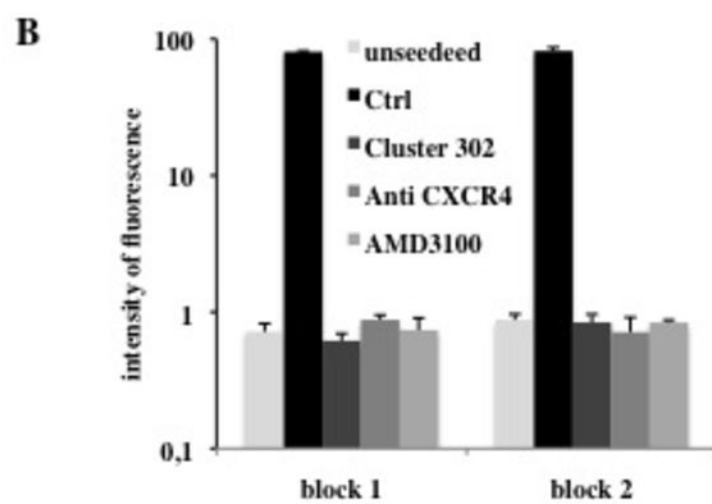
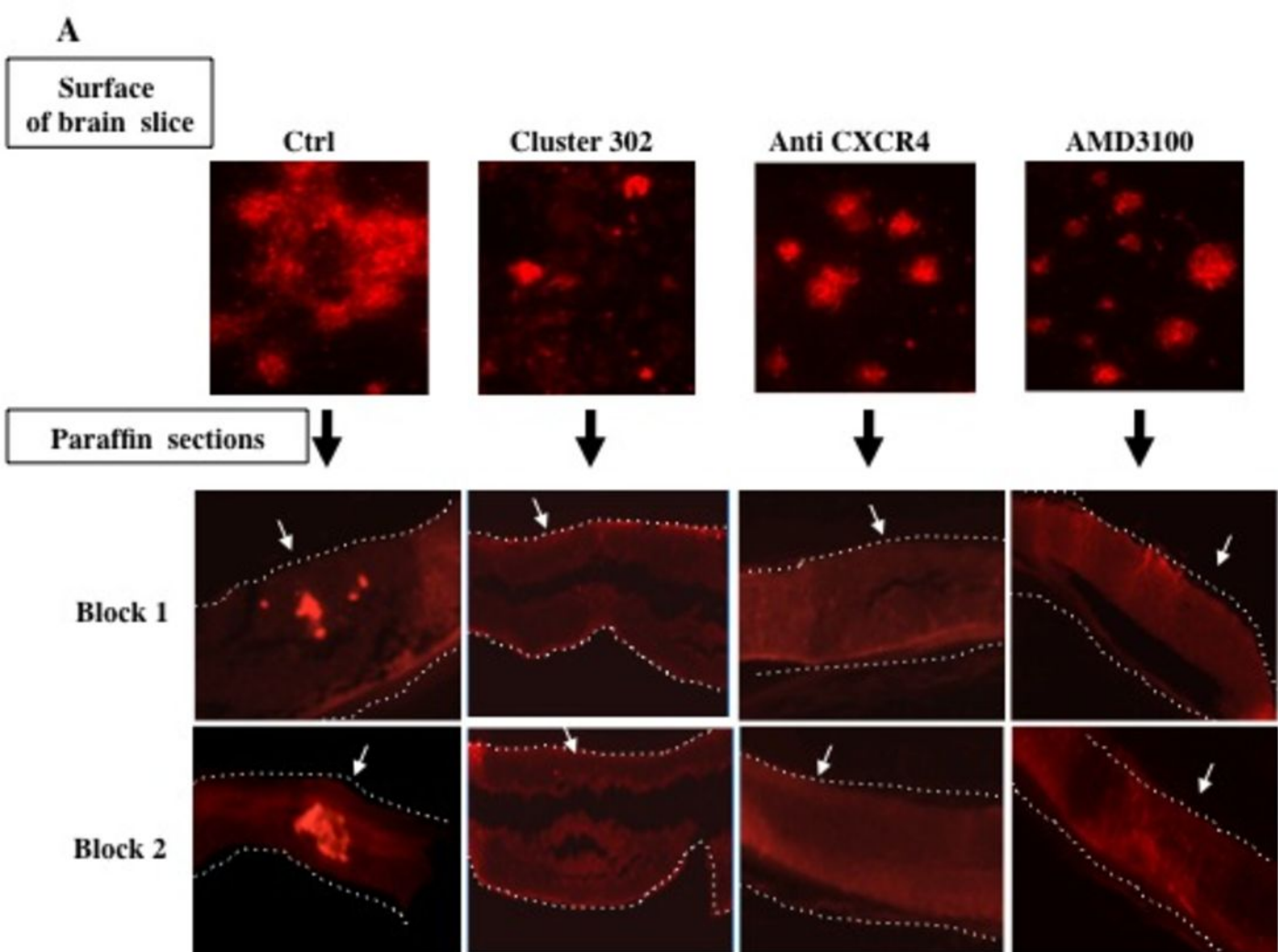


Figure 7

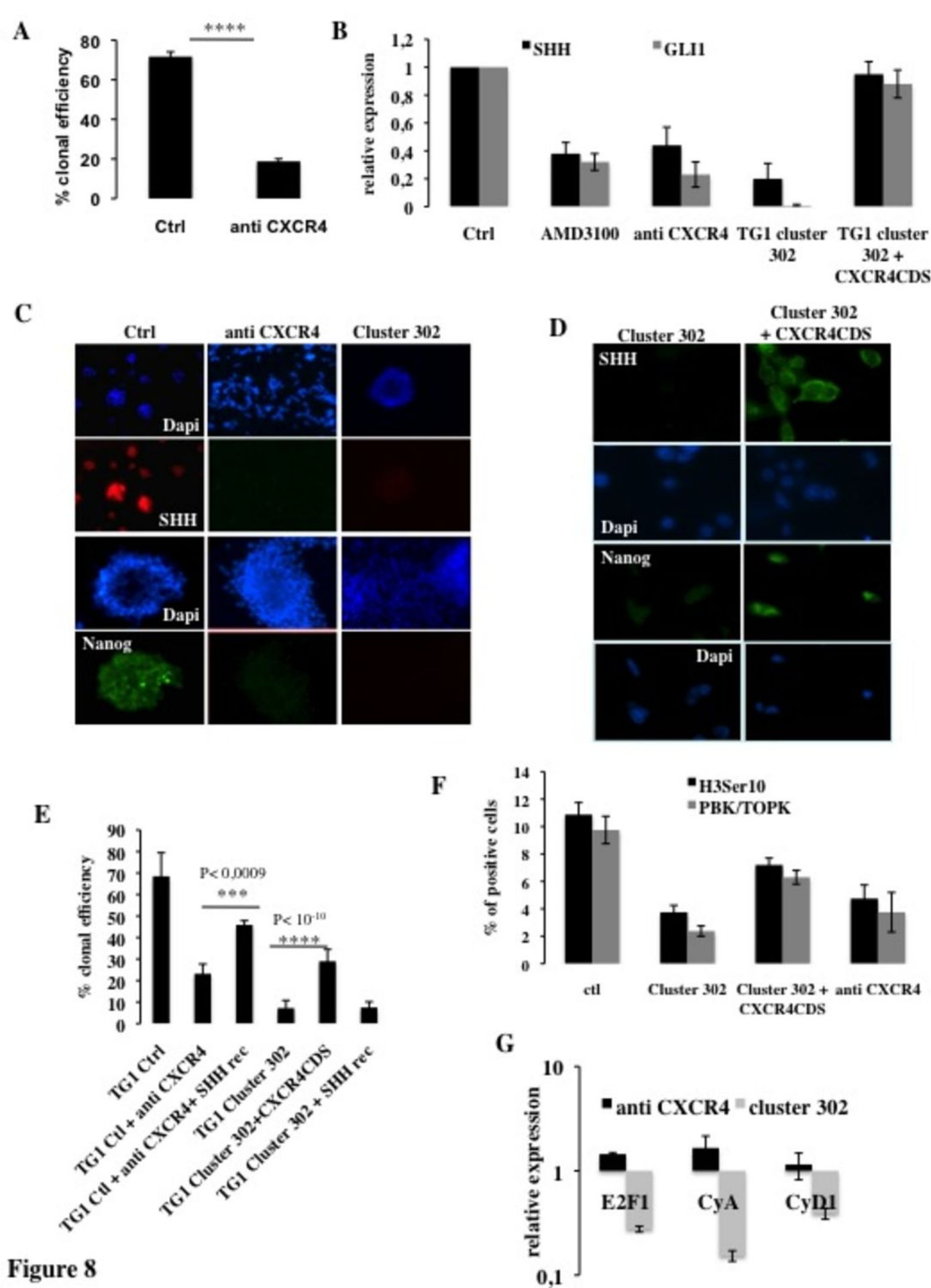


Figure 8